Available online at www.sciencedirect.com

ScienceDirect

Nuclear Physics A 932 (2014) 205–211

NUCLEAR PHYSICS A

www.elsevier.com/locate/nuclphysa

ALICE results on the production of the light-flavor hadrons at the LHC

Jacek Otwinowski for the ALICE Collaboration

Research Division and ExtreMe Matter Institute EMMI, GSI Helmholtzzentrum für Schwerionenforschung, Darmstadt, Germany

Received 11 April 2014; received in revised form 18 September 2014; accepted 18 September 2014

Available online 26 September 2014

Abstract

Production of light-flavor hadrons in pp, p–Pb and Pb–Pb collisions at the LHC has been measured by ALICE. The light-flavor hadrons ($\pi^{\pm}$, $K^{\pm}$, K^0_s, p, $\bar{p}$, Λ, $\bar{\Lambda}$, ϕ) are identified in the various momentum ranges by using specific energy loss (dE/dx), time-of-flight, Cherenkov radiation, and via decay topology and invariant mass analysis for decayed particles. In these proceedings, the p_T spectra, yields and ratios of light-flavor hadrons measured in pp, p–Pb and Pb–Pb collisions in multiplicity (centrality) intervals are presented. The hadron production in different collision systems is compared and confronted with theoretical models.

Keywords: Light-flavor hadrons; Transverse momentum; Nuclear modification factors; Proton–lead collisions; LHC

1. Introduction

Production of light-flavor hadrons is used to study physics phenomena in high energy pp, p–Pb and Pb–Pb collisions at the LHC. In pp collisions, one can study non-perturbative (small Q^2) and perturbative (large Q^2) quantum chromodynamics (QCD) as well as parton fragmentation in the vacuum. The pp is also a reference system for measurements in p–Pb and Pb–Pb collisions.

E-mail address: j.otwinowski@gsi.de (J. Otwinowski).

http://dx.doi.org/10.1016/j.nuclphysa.2014.09.064

In p–Pb collisions, the cold nuclear matter effects (Cronin effect [1], shadowing and gluon saturation [2]) which might influence the particle production at low and high p_{T} are studied. We also search for collective phenomena or indication of the final state effects which might modify hadron spectra. Here, the question is whether the p–Pb can be considered as a reference system for measurements in Pb–Pb collisions.

In Pb–Pb collisions, we try to characterize the quark–gluon plasma (QGP) [3] which is expected to be produced in high energy heavy-ion collisions. At low p_{T}, the main focus is on collective flow. At intermediate p_{T}, the quark recombination (coalescence) can be studied. At high p_{T}, the jet quenching and parton fragmentation in a hot and dense medium can be addressed.

In this proceedings, we present results on primary charged particles (98% hadrons) and identified light-flavor hadrons ($\pi^{\pm}$, $\mathrm{K}^{\pm}$, $\mathrm{K}^{0}_{\mathrm{s}}$, p, $\bar{\mathrm{p}}$, Λ, $\bar{\Lambda}$, ϕ) produced in Pb–Pb at $\sqrt{s_{\mathrm{NN}}} = 2.76$ TeV and p–Pb at $\sqrt{s_{\mathrm{NN}}} = 5.02$ TeV collisions, recorded in 2010–2013. They are compared to results from pp collisions at the LHC. Primary charged particles are defined in ALICE as all charged particles produced in the collision and their decay products, except for particles from weak decays of strange hadrons.

In order to quantify the nuclear effects, particle production in Pb–Pb (p–Pb) to pp is compared with use of the nuclear modification factor

$$R_{\mathrm{PbPb,pPb}}(p_{\mathrm{T}}) = \frac{\mathrm{d}^2 N_{\mathrm{ch}}^{\mathrm{PbPb,pPb}}/\mathrm{d}\eta \mathrm{d}p_{\mathrm{T}}}{\langle N_{\mathrm{coll}}\rangle \mathrm{d}^2 N_{ch}^{\mathrm{pp}}/\mathrm{d}\eta \mathrm{d}p_{\mathrm{T}}}. \tag{1}$$

$N_{\mathrm{ch}}^{\mathrm{PbPb,pPb}}$ and $N_{\mathrm{ch}}^{\mathrm{pp}}$ represent the charged particle yields in Pb–Pb (p–Pb) and in pp collisions. The $\langle N_{\mathrm{coll}}\rangle$ is the average number of binary nucleon–nucleon collisions for a given centrality interval calculated based on Glauber Monte Carlo simulations [4]. The centrality selection is performed only for Pb–Pb collisions [5]. For p–Pb, charged particle yields measured in minimum-bias collisions (no centrality selection) are compared to pp scaled by $\langle N_{\mathrm{coll}}\rangle = A\sigma_{\mathrm{pN}}/\sigma_{\mathrm{pPb}} = 6.9$ with the number of nucleons $A = 208$, proton–nucleon inelastic cross section $\sigma_{\mathrm{pN}} = 70$ mb, and proton–lead inelastic cross section $\sigma_{\mathrm{pPb}} = 2100$ mb. The construction of pp reference spectra is described in [6]. In absence of nuclear modifications, $R_{\mathrm{PbPb,pPb}}$ is equal to unity at high p_{T} where hard processes are dominant.

Data from pp, p–Pb and Pb–Pb collisions are also presented in multiplicity intervals (see [7] for details). Each multiplicity interval corresponds to a different mean charged-particle multiplicity density ($\langle \mathrm{d}N_{\mathrm{ch}}/\mathrm{d}\eta\rangle$) measurement.

2. ALICE experiment

ALICE [8] is a dedicated heavy-ion experiment at the LHC. Fig. 1 shows the ALICE setup where the central barrel is the major detector system for hadron measurements. In the central barrel, there are several detectors which are used for the tracking and/or particle identification. The particle tracks are reconstructed using the hit information from the six silicon layers of the Inner Tracking System (ITS) and up to 159 space points from the Time Projection Chamber (TPC). The relative p_{T} resolution obtained with the ITS and TPC combined tracking amounts to $\sigma_{p_{\mathrm{T}}}/p_{\mathrm{T}} = 1$–$5\%$ for $p_{\mathrm{T}} = 0.1$–20 GeV/c.

ALICE has excellent particle identification (PID) capabilities in the broad transverse momentum range $p_{\mathrm{T}} = 0.1$–20 GeV/c, which is unique at the LHC. Charged hadrons with $p_{\mathrm{T}} = 0.1$–5 GeV/c are identified using the energy loss ($\mathrm{d}E/\mathrm{d}x$) from the ITS and TPC detectors, the

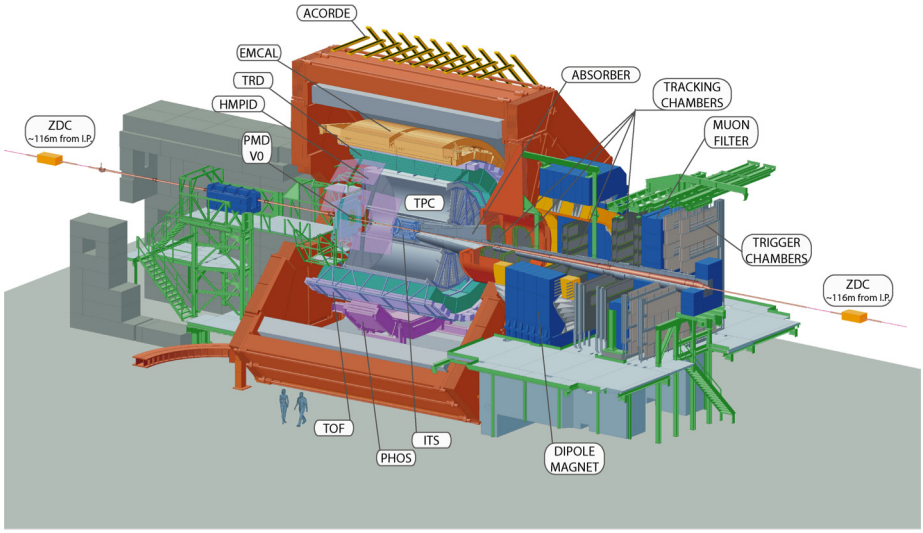

Fig. 1. ALICE setup.

time-of-flight measurement with TOF detector, and Cherenkov light from the high momentum particle identification detector (HMPID). Above $p_{\mathrm{T}} = 5$ GeV/c, they are identified based on the $\mathrm{d}E/\mathrm{d}x$ in the relativistic rise range of the Bethe–Bloch curve in the TPC. The hadrons which decay into charged particles ($\mathrm{K}^0_{\mathrm{s}} \to \pi\pi$, $\Lambda \to \pi p$ and $\phi \to KK$) are identified via their decay topology and invariant mass analysis. In addition, the PID information for their decay products is used to improve the signal to background ratio. More details about tracking and particle identification can be found in [9].

3. Hadron production at low p_{T}

Fig. 2 (left) shows p_{T} spectra of identified hadrons measured in central (0–5%) Pb–Pb collisions [10] in comparison to those at RHIC (STAR [11], PHENIX [12]) and several hydrodynamic models (VISH2 + 1 [13], HKM [14], Kraków [15] and EPOS 2.17 [16]). p_{T} spectra measured at the LHC are harder compared to corresponding spectra at RHIC. The hydrodynamic models describe data well for $p_{\mathrm{T}} < 2$ GeV/c indicating that matter created in such collisions has properties of the strongly coupled liquid which was discovered at RHIC [17]. From the comparison to RHIC and hydrodynamic models one can also conclude that a large radial flow develops in the central Pb–Pb collisions.

Fig. 2 (right) shows p_{T} spectra of identified hadrons measured in high multiplicity p–Pb collisions [7] in comparison to hydrodynamic (Blast-Wave [18], Kraków [19], EPOS LHC [20]) and QCD-inspired (DPMJET [21]) models. The hydrodynamic models describe data reasonably well for $p_{\mathrm{T}} < 2$ GeV/c while the DPMJET failed in describing data for all p_{T}. It might indicate that the collective phenomena (e.g. flow etc.) are present in high multiplicity p–Pb collisions.

p_{T} spectra measured in pp, p–Pb and Pb–Pb collisions are fitted using the blast-wave model [7] and the results are compiled in Fig. 3. The blast-wave fit is performed for multiplicity (pp, p–Pb) or centrality intervals (Pb–Pb). The fit parameters T_{kin} is the kinetic freeze-out temperature and β_{T} is the radial flow velocity. The parameters show a similar trend in p–Pb (increase of β_{T} with multiplicity) as the ones obtained in Pb–Pb. This observation is consistent with the

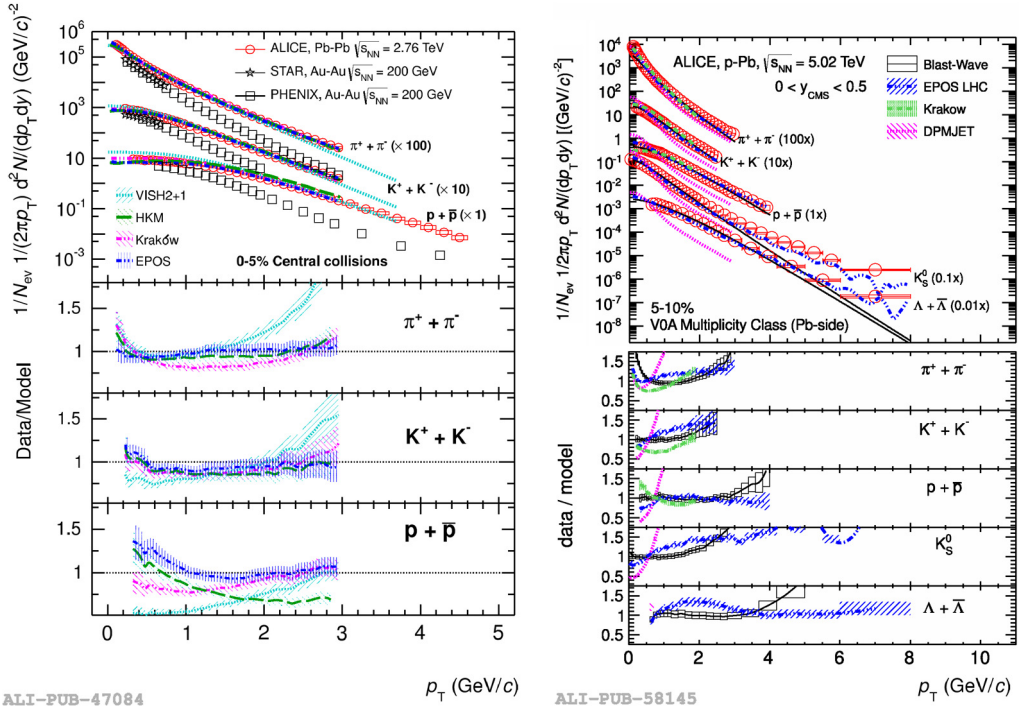

Fig. 2. Left: p_{T} spectra for identified hadrons measured in central (0–5%) Pb–Pb collisions [10] in comparison to measurements at RHIC and models. Right: p_{T} spectra for identified hadrons measured in high multiplicity (5–10%) p–Pb collisions [7] in comparison to models. See text for details.

presence of radial flow in p–Pb collisions. However, a similar trend is visible in pp collisions which might be connected with another source of collectivity (color reconnection [22]) as indicated by PYTHIA8 pp simulations.

4. Hadron production at intermediate p_{T}

Fig. 4 shows p/π (left), $\Lambda/\mathrm{K}^0_{\mathrm{s}}$ (middle) [23] and ϕ/p (right) ratios measured as a function of p_{T} and $\Lambda/\mathrm{K}^0_{\mathrm{s}}$ collision centrality in Pb–Pb collisions. For $p_{\mathrm{T}} < 8$ GeV/c, baryon-to-meson ratio (p/π, $\Lambda/\mathrm{K}^0_{\mathrm{s}}$) increases with collision centrality reaching maximum at $p_{\mathrm{T}} \approx 3$ GeV/c, while ϕ/p ratio (hadrons with similar mass) is almost constant with p_{T} in central Pb–Pb collisions. The ϕ/p ratio indicates that the spectral shape depends on hadron mass rather than on its quark content. This result is different compared to observations at RHIC [24,25] where the ϕ mesons behave rather like $\mathrm{K}^0_{\mathrm{s}}$ than protons or Λ, while comparing nuclear modification factors and elliptic flow coefficients. However, one should note that the radial flow measured at the LHC is stronger than at RHIC and might determine the spectral shapes. Moreover, the constituent quark scaling observed at RHIC does not work at the LHC indicating differences in hadron production mechanisms. Baryon-to-meson ratios are similar in peripheral Pb–Pb and pp collisions. For $p_{\mathrm{T}} > 8$ GeV/c, p/π and $\Lambda/\mathrm{K}^0_{\mathrm{s}}$ are independent of collision centrality and colliding system.

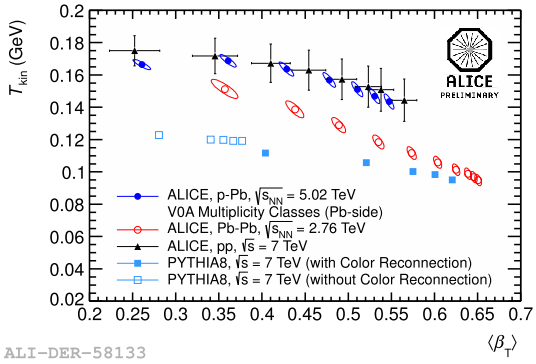

Fig. 3. Results of the blast-wave fits (T_{kin}, $\langle\beta_{\mathrm{T}}\rangle$) to the p_{T} spectra measured in pp, p–Pb and Pb–Pb collisions and from Pythia8 pp simulations.

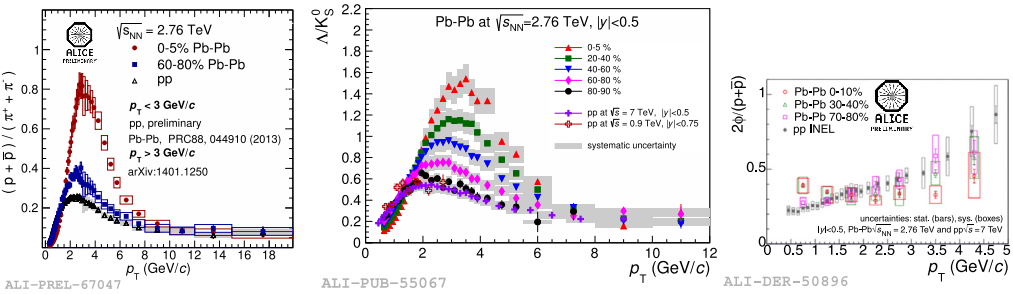

Fig. 4. p/π (left), $\Lambda/\mathrm{K}^0_{\mathrm{s}}$ (middle) [23] and ϕ/p (right) ratios measured as a function of p_{T} and collision centrality in Pb–Pb collisions. For comparison results from pp collisions are also shown.

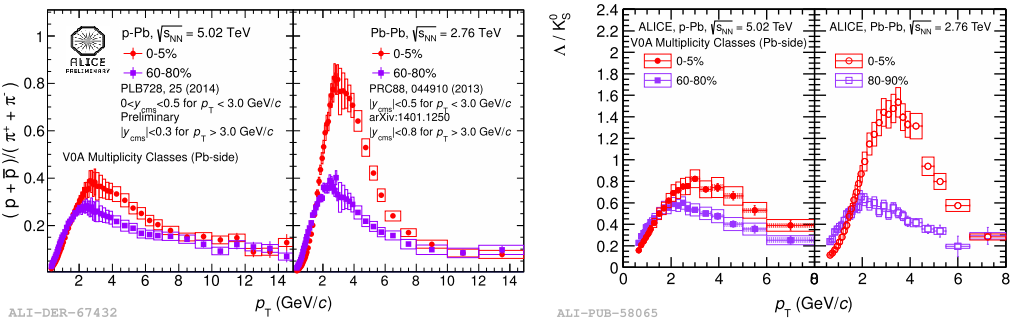

Fig. 5. p/π (left) and $\Lambda/\mathrm{K}^0_{\mathrm{s}}$ (right) [7] ratios measured as a function of p_{T} and event multiplicity in p–Pb collisions. For comparison results from central and peripheral Pb–Pb collisions are shown.

The p/π and $\Lambda/\mathrm{K}^0_{\mathrm{s}}$ [7] ratios have been also measured in p–Pb collisions as a function of multiplicity (Fig. 5). Similar to Pb–Pb, the baryon-to-meson ratio increases with event multiplicity, however, the increase is smaller compared to Pb–Pb which might be due to a smaller radial flow or different particle production mechanisms in these systems.

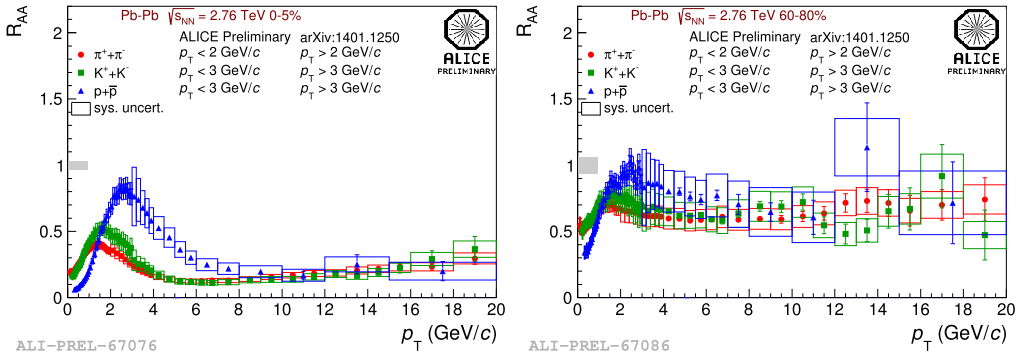

Fig. 6. Nuclear modification factors measured for pions, kaons and protons in central (left) and peripheral (right) Pb–Pb collisions.

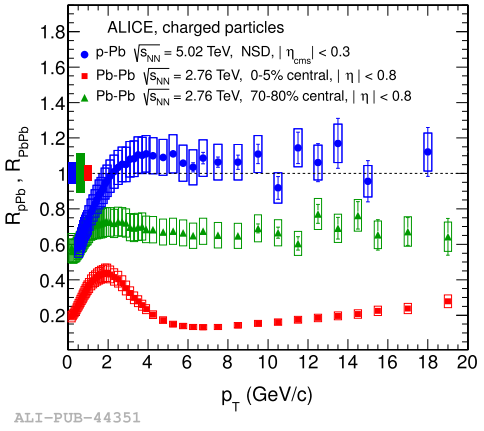

Fig. 7. Nuclear modification factor R_{pPb} for charged particles measured in minimum-bias (no centrality selection) p–Pb collisions [26] in comparison to R_{PbPb} measured in peripheral (70–80%) and central (0–5%) Pb–Pb collisions [27].

5. Hadron production at high p_{T}

Nuclear modification factors R_{PbPb} measured for pions, kaons and protons in central (0–5%) and peripheral (60–80%) Pb–Pb collisions are shown in Fig. 6. A strong suppression of hadron production is observed at high $p_{\mathrm{T}} > 8$ GeV/c (factor 3–5) in central collisions while it is much weaker in peripheral collisions. The suppression at high p_{T} is similar for all hadron species. From these observations, one can conclude that at high p_{T}, the suppression is related to the final state effects (parton interaction with the medium) while parton fragmentation into hadrons is not affected by the medium.

In Fig. 7, nuclear modification factor R_{pPb} for charged particles measured in minimum-bias (no centrality selection), non-single-diffractive (NSD), p–Pb collisions [26] is compared to R_{PbPb} measured in central (0–5%) and peripheral (70–80%) Pb–Pb collisions [27]. For $p_{\mathrm{T}} > 2$ GeV/c, R_{pPb} is consistent with unity which indicates that the suppression of particle production observed in Pb–Pb collisions is related to final state effects.

6. Summary

A strong radial flow is observed in central Pb–Pb collisions at the LHC. There is also indication of the radial flow in high multiplicity p–Pb collisions, however, it might be also related to other collective phenomena (e.g. color reconnection). From baryon-to-meson ratios measured in Pb–Pb and p–Pb collisions one can conclude that the spectral shape depends on hadron mass rather than its quark content. The baryon-to-meson ratio in high-multiplicity p–Pb collisions is much smaller compared to central Pb–Pb collisions which might be due to a smaller radial flow or different particle production mechanisms (e.g. via coalescence). Suppression of hadron production at high p_{T} in Pb–Pb collisions is due to final state effects while parton fragmentation is not affected by the medium at high p_{T}.

References

[1] J.W. Cronin, et al., Phys. Rev. D 11 (1975) 3105.
[2] C. Salgado, et al., J. Phys. G 39 (2012) 015010.
[3] B. Muller, J. Schukraft, B. Wyslouch, Annu. Rev. Nucl. Part. Sci. 62 (2012) 361.
[4] M. Miller, et al., Annu. Rev. Nucl. Part. Sci. 57 (2007) 205.
[5] B. Abelev, et al., ALICE Collaboration, Phys. Rev. C 88 (2013) 044909.
[6] B. Abelev, et al., ALICE Collaboration, Eur. Phys. J. C 73 (2013) 2662.
[7] B. Abelev, et al., ALICE Collaboration, Phys. Lett. B 728 (2014) 25.
[8] K. Aamodt, et al., ALICE Collaboration, J. Instrum. 3 (2008) S08002.
[9] B. Abelev, et al., ALICE Collaboration, arXiv:1402.4476, 2014.
[10] B. Abelev, et al., ALICE Collaboration, Phys. Rev. C 88 (2013) 044910.
[11] B. Abelev, et al., STAR Collaboration, Phys. Rev. C 79 (2009) 034909.
[12] S.S. Adler, et al., PHENIX Collaboration, Phys. Rev. C 69 (2004) 034909.
[13] C. Shen, et al., Phys. Rev. C 84 (2011) 044903.
[14] I. Karpenko, Y. Sinyukov, K. Werner, Phys. Rev. C 87 (2013) 024914.
[15] P. Bozek, I. Wyskiel-Piekarska, Phys. Rev. C 85 (2012) 064915.
[16] K. Werner, et al., Phys. Rev. C 85 (2012) 064907.
[17] I. Arsene, BRAHMS Collaboration, Nucl. Phys. A 757 (2005) 1;
B.B. Back, et al., PHOBOS Collaboration, Nucl. Phys. A 757 (2005) 28;
J. Adams, et al., STAR Collaboration, Nucl. Phys. A 757 (2005) 102;
K. Adcox, PHENIX Collaboration, Nucl. Phys. A 757 (2005) 184.
[18] P. Huovinen, et al., Phys. Lett. B 503 (2001) 58.
[19] P. Bozek, Phys. Rev. C 85 (2012) 014911.
[20] T. Pierog, et al., arXiv:1306.0121 [hep-ph], 2013.
[21] S. Roesler, R. Engel, J. Ranft, arXiv:hep-ph/0012252, 2000.
[22] A. Ortiz Velasquez, et al., Phys. Rev. Lett. 111 (2013) 042001.
[23] B. Abelev, et al., ALICE Collaboration, Phys. Rev. Lett. 111 (2013) 222301.
[24] B.I. Abelev, et al., STAR Collaboration, Phys. Rev. C 79 (2009) 064903.
[25] A. Adare, et al., PHENIX Collaboration, Phys. Rev. C 83 (2011) 024909.
[26] B. Abelev, et al., ALICE Collaboration, Phys. Rev. Lett. 110 (2013) 082302.
[27] B. Abelev, et al., ALICE Collaboration, Phys. Lett. B 720 (2013) 52.